

This is the **Accepted Version** of the manuscript published as article in
Low Temperature Physics, to be cited as follows:

The effect of graphene oxide reduction temperature on the kinetics of low-
temperature sorption of hydrogen

A. V. Dolbin, N. A. Vinnikov, V. B. Esel'son, V. G. Gavrilko, R. M.
Basnukaeva, M. V. Khlistuck, W. K. Maser, and A. M. Benito

Low Temp. Phys. 45, 422 (2019)

Published Online: 03 April 2019

DOI: <https://doi.org/10.1063/1.5093523>

The effect of graphene oxide reduction temperature on the kinetics of low-temperature sorption of hydrogen

A. V. Dolbin,^{1,a)} N. A. Vinnikov,¹ V. B. Esel'son,¹ V. G. Gavrillo,¹ R. M. Basnukaeva,¹
M. V. Khlistuck,¹ W. K. Maser,² and A. M. Benito²

¹B. Verkin Institute for Low Temperature Physics and Engineering of the National
Academy of Sciences of Ukraine, 47 Nauky Ave., Kharkiv 61103, Ukraine

²Instituto de Carboquímica, 4 Miguel Luesma Castán, Zaragoza E-50018, Spain

ABSTRACT

The effect of thermal reduction of graphene oxide on the hydrogen sorption and desorption kinetics was studied by temperature-programmed desorption in the 7–120 K temperature range. The heat treatment of graphene oxide samples resulted in a decrease in the activation energy for hydrogen diffusion by more than an order of magnitude (by a factor of 12–13) compared with the initial graphite oxide. This change in the activation energy is, most likely, caused by exfoliation (loosening) of the graphite oxide carbon sheets upon the thermal removal of intercalated water, which changes the sorption character by decreasing the influence of the opposite walls in the interlayer spaces.

1. INTRODUCTION

Currently, hydrogen is considered to be the most promising environmentally clean fuel. First of all, this is due to the high energy content of hydrogen fuel (142MJ/kg), which is three times greater than that of oil; furthermore, hydrogen is converted to steam upon combustion. Today, hydrogen fuel cells are among the most promising sources of environmentally clean electrical energy. The progress of hydrogen-based power engineering requires well-developed technologies of hydrogen fuel production, accumulation, storage, and transportation. In light of this, the search for methods and materials suitable for efficient reversible hydrogen storage assumes a key significance. During the last decade, potential hydrogen storage materials such as organometallic structures, carbon-based activated metal hydride compounds,^{1,2} and others, have been studied in detail. However, a number of fundamental drawbacks (such as the insufficient hydrogen concentration in the storage material and its low durability) still preclude the manufacture of hydrogen storage systems suitable for industrial use based on these materials.

Carbon nanomaterials are fairly promising sorbents, particularly for the sorption of gases, as they have cavities that are commensurate with gas particles. In quite a few studies devoted to elucidating the mechanisms and conditions for optimal hydrogen storage in carbon nanostructures (fullerite, nanotubes), the average energy of hydrogen sorption by these structures was found to be 0.2–0.4 eV/mol (19.3–38.6 kJ/mol).³ These energy values are intermediate between the energies of physical and chemical sorption.⁴ The discovery and study of the properties belonging to monolayer carbon, graphene,⁵ initiated extensive research of the unusual physical properties of this material, which revealed new potential opportunities for gas storage. The calculated limiting binding energies and mass concentrations of hydrogen in graphene for physisorption were

0.015–0.06 eV^{6,7} and 3.3%³ (6.6% for double-sided sorption), respectively. In the case of molecular hydrogen chemisorption, the energy needed for covalent bond formation is ~ 1.5 eV.⁸ This value includes the hydrogen dissociation energy (dissociative adsorption). The chemisorption of atomic hydrogen on a carbon sheet is energetically more favorable: the C–H bond energy is ~ 0.7 eV and the chemisorption barrier is ~ 0.3 eV.^{9,10} The theoretical limit for the mass concentration of hydrogen chemisorbed on graphene is 8.3%, which corresponds to one hydrogen atom linked to each graphene carbon atom (1/12), or to so-called graphane.^{11,12} However, the removal of hydrogen chemically bound to graphene can be performed only by heating to a high temperature (at least 450 °C¹² and can give rise to defects and carbon sheet destruction.

Real graphene-based materials usually consist of several carbon sheets connected by weak van der Waals interactions. A characteristic example of such material is graphene oxide, which is prepared by chemical oxidation of graphite^{13–15} with subsequent exfoliation by way of ultrasonic or chemical treatment, or by thermal heating. The final sorption properties of graphene materials depend on the type, number, and distribution of oxygen functional groups on the graphene surface, and on the number and type of defects generated upon removal of these groups. These characteristics depend, in turn, on the reduction technique. The exfoliation of graphite oxide by thermal heating is due to the fast removal of water, intercalated during oxidation, and oxygen-containing groups from interlayer spaces. This spontaneous intense process results in increasing pressure between close-packed graphite oxide layers, which promotes exfoliation of the carbon sheets. The material thus obtained, thermally reduced graphene oxide (TRGO), consists of grains comprising up to ten carbon sheets with an interlayer spacing of 6–8 Å. The thermal reduction of graphene oxide has some advantages over chemical reduction techniques. First, using controlled

heating, it is possible to manage the numbers of oxygen functional groups and structural defects, as well as the sorption characteristics of graphene oxide samples. It is known that structural defects can cause at least a two-fold increase in the graphene area accessible for sorption.^{16,17} Furthermore, thermal heating does not imply the use of reducing agents and therefore rules out the appearance of chemical impurities on the graphene surfaces.

This article considers how the sample reduction temperature (heat treatment) impacts the kinetics of low-temperature hydrogen sorption.

2. RESEARCH METHODS AND TEST SAMPLES

The kinetics of hydrogen gas sorption and desorption by the initial graphite oxide (GtO) and thermally reduced graphene oxide (TRGO) were studied in the temperature range of 7–120 K by measuring the time dependences of the gas pressure in contact with the test sample in a closed space (temperature-programmed desorption). The research methods and the experimental equipment have previously been described in detail in Refs. 18–20. The initial graphite oxide, which was subsequently heat-treated to prepare graphene oxide, was obtained by a modified Hummers method^{13,21} from a graphite powder (Sigma-Aldrich) using strong oxidants (NaNO_3 , H_2SO_4 , and KMnO_4). The procedure used to manufacture the initial graphite oxide powder (hereinafter referred to as GtO) was described in Ref. 17. The thermal exfoliation of the graphite oxide powder thus obtained was carried out for five samples at different temperatures (200, 300, 500, 700, and 900 °C) for 15 min under argon. The resulting graphene-based materials were designated as TRGO-200, TRGO-300, TRGO-500, TRGO-700, and TRGO-900. The initial graphite oxide and the heat-treated samples were thoroughly investigated by X-ray spectroscopy and electron microscopy.²² It was found that

heating of graphite oxide samples to 200 °C induces intense vaporization of water intercalated between graphite sheets during sample manufacture. Fast water vaporization results in the exfoliation of graphite oxide, i.e., sharp increase in the distance between the carbon sheets, which markedly increases the sorption capacity of the material.¹⁷ Heating above 200 °C initiates two competing processes that determine the features of the sample structure: the reduction of the graphite carbon structure, which decreases the interlayer spacing via removal of oxygen-containing groups and mechanical stress relaxation, and the formation of defects via detachment of carbon atoms directly coupled with oxygen atoms in oxygen-containing groups by strong covalent bonds. The latter of the above-mentioned factors has the most pronounced effect on the structure and sorption properties of the sample heat-treated at the highest temperature of 900 °C.¹⁷ The previous studies of the low-temperature hydrogen sorption–desorption by thermally reduced graphene oxide²³ revealed that the highest sorption capacity exists for samples treated at 300 and 900 °C (**Fig. 1**).

Prior to the measurements, each sample was evacuated for four days directly in the measuring cell to remove the possible impurity gases. The remaining moisture was removed by periodically cleansing the cell with pure nitrogen. The samples were saturated with standard hydrogen with a 99.98% purity (impurity contents: $O_2 \leq 0.01\%$ and $N_2 \leq 0.01\%$). Hydrogen saturation of carbon nanomaterial samples was performed at pressures of ~ 1 Torr. The lowest measurement temperature is caused by the minimum saturated vapor pressure of hydrogen accessible for measurements: at 7 K, the equilibrium hydrogen vapor pressure is $\sim 1.3 \times 10^{-3}$ Torr. The saturation and desorption took place at a constant specified sample temperature. The variation of the gas pressure in the closed cell containing the sample during saturation or desorption was measured by MKS Baratron capacitance pressure sensors, with the minimum measurable pressure

being 1×10^{-4} Torr. The error of pressure measurement was not more than 0.12% of the measured value. After completion of sorption, the cell was sealed and the pressure variation during desorption of the admixture from the powder during its stepwise heating was recorded. The H_2 gas released upon heating was withdrawn in portions into an evacuated calibrated vessel. The gas withdrawal from the samples lasted until the gas pressure above the sample decreased to 10^{-2} Torr. After completion of desorption at a specified temperature, the sample temperature was changed to the next specified value and the desorption step was repeated.

3. RESULTS AND DISCUSSION

The kinetics of hydrogen sorption and subsequent desorption for the initial graphite oxide and thermally reduced graphene oxide at different reduction temperatures were measured in the temperature range of 7–120 K. The resulting time dependences of H_2 pressure in the cell during sorption or desorption are well described by the exponential function with a single parameter (τ) (see Fig. 2).

$$\Delta P = A[1 - \exp(-t/\tau)]. \quad (1)$$

At a constant temperature, characteristic times of sorption and desorption for the same sample coincided within experimental error. The characteristic times of hydrogen diffusion in GtO and TRGO samples could be affected by interconversion between ortho and para-spin isomers of H_2 molecules. In order to eliminate this effect from the measurement results, the procedure provided for the measurement of the characteristic sorption and desorption times to be done over short periods of time in which the nuclear spin conversion could hardly have time to occur.²⁵ **Figure 3** shows the temperature dependences of the characteristic times of H_2 sorption (desorption) by a graphite oxide sample [Fig. 3(a)], and by thermally reduced TRGO samples [Figs. 3(a) and 3(b)].

Note that over the whole temperature range used in experiments, the error of measurements caused by the intrinsic time needed for the gas phase present in the system to reach thermal equilibrium (thermalization time) was at least an order of magnitude smaller for all samples than the measured characteristic times.

As the temperature was reduced from 50 K to approximately 30–40 K, the hydrogen sorption times increased for all samples [Figs. 3(a) and 3(b)]. This type of dependence indicates that the sorption behavior in this temperature range is mainly determined by thermally activated diffusion of H₂ molecules. As the temperature was further reduced, the sorption times tended to decrease [Fig. 3(b)]. At temperatures below 20 K, the characteristic times of H₂ sorption depended only slightly on the temperature [Figs. 3(a) and 3(b)]. These features of the temperature dependence of hydrogen sorption times suggest that at temperatures below 20 K, tunneling of H₂ molecules between the graphene oxide carbon sheets is the predominant diffusion process determining the sorption (desorption) rate. Thus, non-monotonic temperature dependences of the characteristic times of hydrogen sorption by GtO and TRGO samples are, most likely, caused by competition of the thermally activated diffusion, which dominates at temperatures above 40 K, and tunneling diffusion, which prevails at low temperatures. Similar effects have already been observed previously in a study of gas sorption by fullerite C₆₀, singlewalled carbon nanotubes,^{18,24,26} and chemically reduced graphene oxide.²⁷ The abnormal behavior of H₂ diffusion coefficients at temperatures below 10 K for GtO and TRGO samples can be attributed to the capillary condensation of H₂ molecules in interlayer spaces.

The obtained characteristic times τ were used to estimate the diffusion coefficients for hydrogen into graphite oxide, and thermally reduced graphene oxide:

$$D \approx \frac{\bar{l}^2}{4 \pi \tau}, \quad (2)$$

where \bar{l} is the average grain (granule) size of GtO and TRGO powders ($\sim 10 \mu\text{m}$);²² τ is the characteristic time of diffusion.

Presumably, filling of the grains of graphene oxide powder with H_2 molecules occurred mainly along the carbon sheets. Therefore, the proportionality factor for the near-two-dimensional case of diffusion, which appears in the denominator of relation (2), was taken to be approximately four.

In order to determine the activation energy (E_a) for hydrogen diffusion in graphene oxide, the temperature dependence of the diffusion coefficients was plotted in the $Y = \ln(D) - X = 1/T$ coordinates (a typical example for GtO and TRGO-200 samples is given in **Fig. 4**). The activation energy was determined by a linear approximation of experimental data for $Y = \ln(D)$ versus $X = 1/T$ (3) of the thermally activated segment for each reduction temperature.

$$D = D_0 \exp\left(-\frac{E_a}{k_B T}\right), \quad (3)$$

where D_0 is the pre-exponential factor depending on the frequency of collisions between the admixture molecules and the matrix; k_B is the Boltzmann constant. It should be noted that in the relation $\ln(D)(1/T)$, we observed no anomalies similar to those found previously for the behavior of ^4He diffusion coefficients in thermally reduced graphene oxide samples.²² These anomalies may have been associated with the ^4He admixture atoms' transition into the two-dimensional quantum liquid state. Presumably, no phenomena of this type are involved in the sorption of molecular hydrogen by graphene oxide in the temperature range we considered.

The dependence of the hydrogen diffusion activation energy on the heat treatment temperature of the GtO and TRGO samples is presented in **Fig. 5** and in **Table I**.

It is worth noting that the obtained activation energies are consistent with

published data on the energy of hydrogen physisorption by multilayer graphene.⁷

Attention is drawn by the non-monotonic dependence of the activation energy on the heat treatment temperature of graphene oxide samples. It is known from X-ray diffraction²² and Raman spectroscopy data¹⁷ that heating the samples up to 200 °C induces intense vaporization of water intercalated between carbon sheets, and exfoliation of the sheets into single flakes.²⁸ Since this considerably decreases the number of interlayer cavities and the influence of the second cavity wall on H₂ molecules, the activation energy for hydrogen diffusion in the sample treated at 200 °C sharply decreases as compared with that for the initial graphite oxide (**Fig. 5**). Heating the samples to higher temperatures brings about several processes that influence the kinetics of hydrogen sorption by thermally reduced samples. First, oxygen-containing groups are eliminated, resulting in the neighboring graphene flakes sticking together again under the action of van der Waals forces.^{17,29} Furthermore, heating facilitates the relaxation of mechanical stress and the smoothing of wrinkles.¹⁷ These phenomena promote the restoration of the initial layered structure of graphene oxide and somewhat increase the activation energy (see **Fig. 5**, reduction temperature of 300 °C). Meanwhile, the removal of oxygen-containing groups leads to the detachment of carbon atoms from the sheets and the formation of defects, which exposes additional surface sites and sorption paths and, hence, somewhat decreases the activation energy (for the sample thermally reduced at 700 °C, **Fig. 5**). In the case of a sample treated at 900 °C, the effect of restoration of the layered structure and graphitization proved to be the dominant, which results in increasing activation energy. Thus, the heating of graphite oxide samples above 200 °C induces two competing processes that determine the type of temperature dependence the hydrogen diffusion coefficients in the treated samples will have: restoration of the graphite carbon structure, which increases the activation energy,

and defect formation, which decreases the activation energy. As a result, the dependence of the activation energy for hydrogen diffusion on the temperature of thermal reduction of graphene oxide is non-monotonic (**Fig. 5**).

The dependence of the activation energy for hydrogen diffusion on the temperature of sample treatment, obtained by temperatureprogrammed desorption, correlates with the change in the amount of crystalline graphite oxide phase with increasing annealing temperature.²² It is also noteworthy that the dependence $E_a(T)$ is in qualitative agreement with the activation energy values determined previously for helium diffusion²² (**Fig. 5**). The substantial quantitative differences in the hydrogen and helium E_a values for the initial graphite oxide and the sample with the highest temperature of heat treatment are due, most likely, to specific features of the interaction between the carbon sheets and admixture particles (the calculated interaction energy between the molecular hydrogen and graphene is 0.015–0.06 eV;^{6,7} and for helium and graphene it is 0.011 eV.³⁰

4. CONCLUSION

The thermal reduction of graphene oxide had a considerable effect on the kinetics of low-temperature sorption of hydrogen by heat-treated samples, and resulted in a more than an order of magnitude (by a factor of 12–13) decrease in the activation energy for hydrogen diffusion, as compared with the activation energy for the initial graphite oxide. This change in the activation energy can be attributed to exfoliation of the graphite oxide carbon sheets by the thermal removal of the intercalated water, which actually changes the sorption character by decreasing the influence of the opposite wall in the interlayer space.

ACKNOWLEDGMENTS

The authors are grateful to Prof. A.I. Prokhvatilov for the fruitful discussion of the results of the study, and to the National Academy of Sciences of Ukraine for the financial support within the framework of the program “Fundamental Problems of the Development of New Nanomaterials and Nanotechnologies” (Project No. 0115U001397).

REFERENCES

- ¹Y. Gogotsi, R. K. Dash, G. Yushin, T. Yildirim, G. Laudisio, and J. E. Fischer, *J. Am. Chem. Soc.* 127, 16006 (2005).
- ²T. Yildirim and S. Ciraci, *Phys. Rev. Lett.* 94, 175501 (2005).
- ³A. Züttel, P. Sudan, Ph. Mauron, T. Kiyobayashi, Ch. Emmenegger, and L. Schlapbach, *Int. J. Hydrogen Energy* 27, 203 (2002).
- ⁴M. Ritschel, M. Uhlemann, O. Gutfleisch, A. Leonhardt, A. Graff, and C. Taschner, *App. Phys. Lett.* 80, 2985 (2002).
- ⁵K. S. Novoselov, A. K. Geim, S. V. Morozov, D. Jiang, Y. Zhang, S. V. Dubonos, I. V. Grigorieva, and A. A. Firson, *Science* 306, 666 (2004).
- ⁶V. Tozzini and V. Pellegrini, *J. Phys. Chem. C* 115, 25523 (2011).
- ⁷S. Patchkovskii, J. S. Tse, S. N. Yurchenko, L. Zhechkov, T. Heine, and G. Seifer, *PNAS* 102, 10439 (2005).
- ⁸Y. Miura, W. Dino, and H. Nakanishi, *J. Appl. Phys.* 93, 3395 (2003).
- ⁹T. Zecho, A. Güttler, X. Sha, B. Jackson, and J. Küppers, *J. Chem. Phys.* 117, 8486 (2002).
- ¹⁰L. Jeloica and V. Sidis, *Chem. Phys. Lett.* 300, 157 (1999).
- ¹¹J. O. Sofo, A. S. Chaudhari, and G. D. Barber, *Phys. Rev. B* 75, 153401 (2007).

- ¹²D. C. Elias, R. R. Nair, T. M. G. Mohiuddin, S. V. Morozov, P. Blake, M. P. Halsall, A. C. Ferrari, D. W. Boukhvalov, M. I. Katsnelson, A. K. Geim, and K. S. Novoselov, *Science* 323, 610 (2009).
- ¹³W. S. Hummers and R. E. Offermann, *J. Am. Chem. Soc.* 80, 1339 (1958).
- ¹⁴D. C. Marcano, D. V. Kosynkin, J. M. Berlin, A. Sinitskii, Z. Z. Sun, A. Slesarev, L. B. Alemany, W. Lu, and J. M. Tour, *ACS Nano* 4, 4806 (2010).
- ¹⁵L. Staudenmaier, *Chem. Ber.* 31, 1481 (1898).
- ¹⁶I. A. Baburin, A. Klechikov, G. Mercier, A. Talyzin, and G. Seifert, *Int. J. Hydrogen Energy* 40, 6594 (2015).
- ¹⁷A. V. Dolbin, M. V. Khlistyuck, V. B. Esel'son, V. G. Gavrillo, N. A. Vinnikov, R. M. Basnukaeva, I. Maluenda, W. K. Maser, and A. M. Benito, *Apl. Surf. Science* 361, 213 (2016).
- ¹⁸A. V. Dolbin, V. B. Esel'son, V. G. Gavrillo, V. G. Manzhelii, N. A. Vinnikov, and S. N. Popov, *JETP Lett.* 93, 577 (2011).
- ¹⁹A. V. Dolbin, V. B. Esel'son, V. G. Gavrillo, V. G. Manzhelii, N. A. Vinnikov, and S. N. Popov, *Fiz. Nizk. Temp.* 36, 1352 (2010) [*Low Temp. Phys.* 36, 1091 (2010)].
- ²⁰A. V. Dolbin, V. B. Esel'son, V. G. Gavrillo, V. G. Manzhelii, N. A. Vinnikov, S. N. Popov, N. I. Danilenko, and B. Sundqvist, *Fiz. Nizk. Temp.* 35, 613 (2009) [*Low Temp. Phys.* 35, 484 (2009)].
- ²¹C. Valles, J. David Nunez, A. M. Benito, and W. K. Maser, *Carbon* 50, 835 (2012).
- ²²A. V. Dolbin, M. V. Khlistuck, V. B. Esel'son, V. G. Gavrillo, N. A. Vinnikov, R. M. Basnukaeva, A. I. Prokhvatilov, I. V. Legchenkova, V. V. Meleshko, W. K. Maser, and A. M. Benito, *Fiz. Nizk. Temp.* 43, 471 (2017) [*Low Temp. Phys.* 43, 383 (2017)].
- ²³O. V. Dolbin, V. B. Esel'son, V. G. Gavrillo, V. G. Manzhelii, M. A. Vinnikov, M. V. Khlistyuk, R. M. Basnukaeva, W. K. Maser, and A. Benito, *J. Nano-Electron. Phys.* 7

(2015).

²⁴B. A. Danilchenko, I. I. Yaskovets, I. Y. Uvarova, A. V. Dolbin, V. B. Esel'son, R. M. Basnukaeva, and N. A. Vinnikov, *Appl. Phys. Lett.* 104, 173109 (2014).

²⁵A. V. Dolbin, M. V. Khlistyuk, V. B. Esel'son, V. G. Gavrilko, M. A. Vinnikov, and R. M. Basnukaeva, *Fiz. Nizk. Temp.* 42, 1455 (2016) [*Low Temp. Phys.* 42, 1139 (2016)].

²⁶A. V. Dolbin, V. B. Esel'son, V. G. Gavrilko, V. G. Manzhelii, N. A. Vinnikov, R. M. Basnukaeva, I. I. Yaskovets, I. Yu. Uvarova, and B. A. Danilchenko, *Fiz. Nizk. Temp.* 40, 317 (2014) [*Low Temp. Phys.* 40, 246 (2014)].

²⁷A. V. Dolbin, V. B. Esel'son, V. G. Gavrilko, V. G. Manzhelii, N. A. Vinnikov, R. M. Basnukaeva, V. V. Danchuk, N. S. Mysko, E. V. Bulakh, W. K. Maser, and A. M. Benito, *Fiz. Nizk. Temp.* 39, 1397 (2013) [*Low Temp. Phys.* 39, 1090 (2013)].

²⁸S. H. Huh, *InTech*, CC BY-NC-SA (2011).

²⁹M. Acik, G. Lee, C. Mattevi, A. Pirkle, R. M. Wallace, M. Chhowalla, K. Cho, and Yv. Chabal, *J. Phys. Chem. C* 115, 19761 (2011).

³⁰T. L. Badman and J. M. McMahon, *Crystals* 8, 202 (2018).

TABLES

TABLE I. The activation energy for the hydrogen diffusion in grpahite oxide (GtO) and thermally reduced graphene oxide (TRGO)

Sample	GtO	TRGO-200	TRGO-300	TRGO-500	TRGO-700	TRGO-900
Activation energy E_a , K	275.5	21.34	27.73	23.23	19.95	76.67

FIGURES

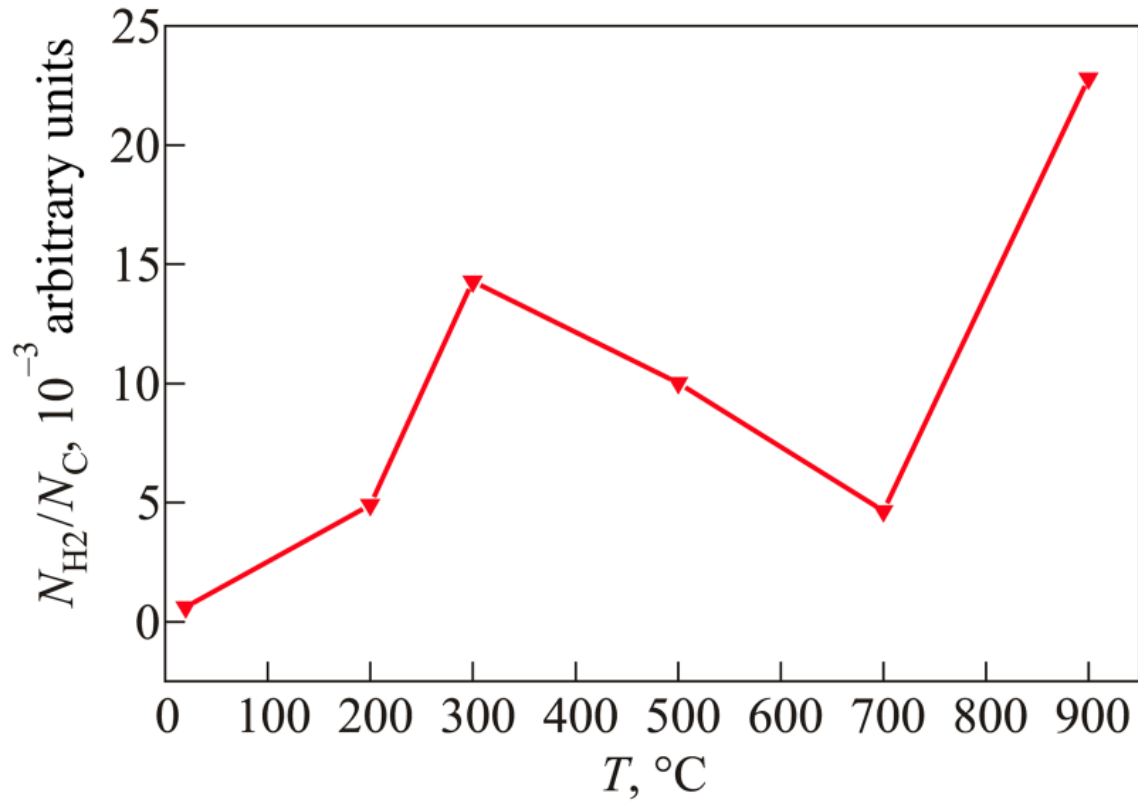


FIG. 1. Temperature dependence of the relative amount of hydrogen NH_2/NC (NH_2 is the number of hydrogen molecules, NC is the number of carbon atoms in the sample) desorbed from GtO and TRGO samples at different reduction temperatures.²³

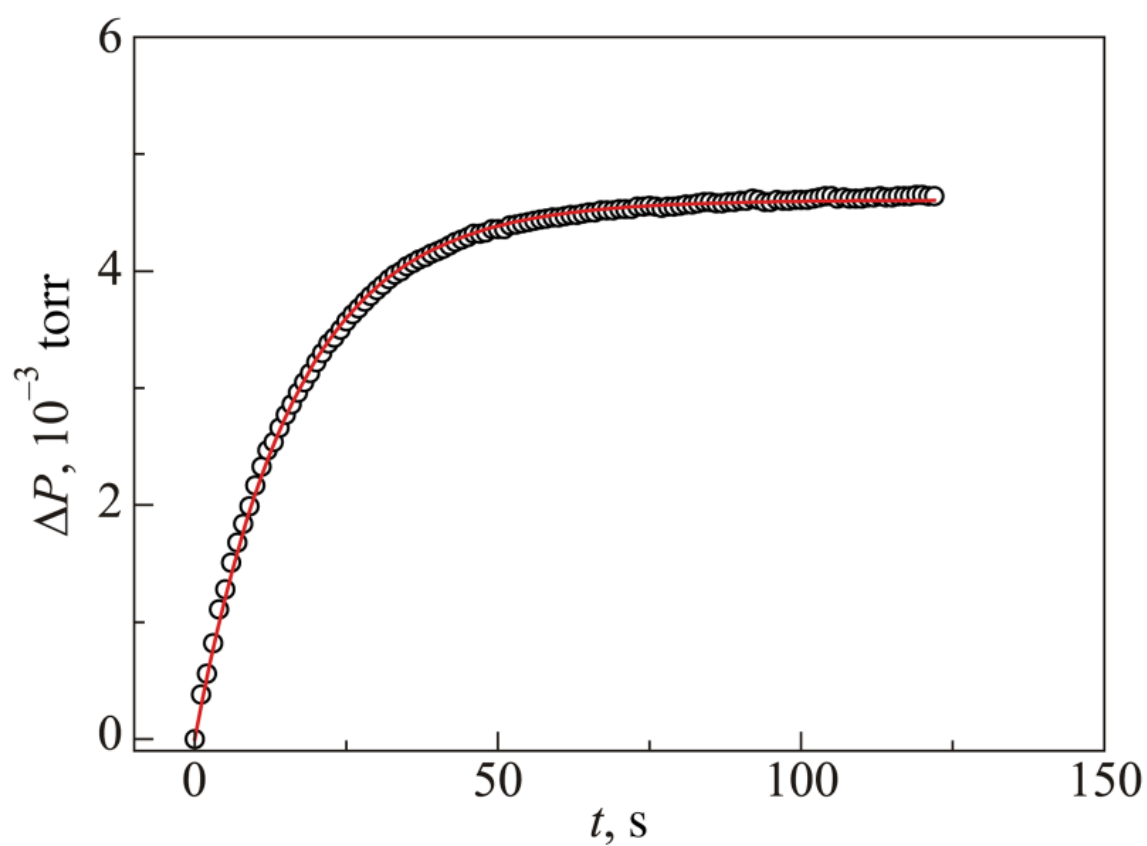


FIG. 2. Experimental data for pressure variation during H₂ desorption from a graphene oxide sample reduced at 200 °C (TRGO-200) (symbols), and the results of data description by an exponential function (line) (exemplified by values obtained at 12 K).

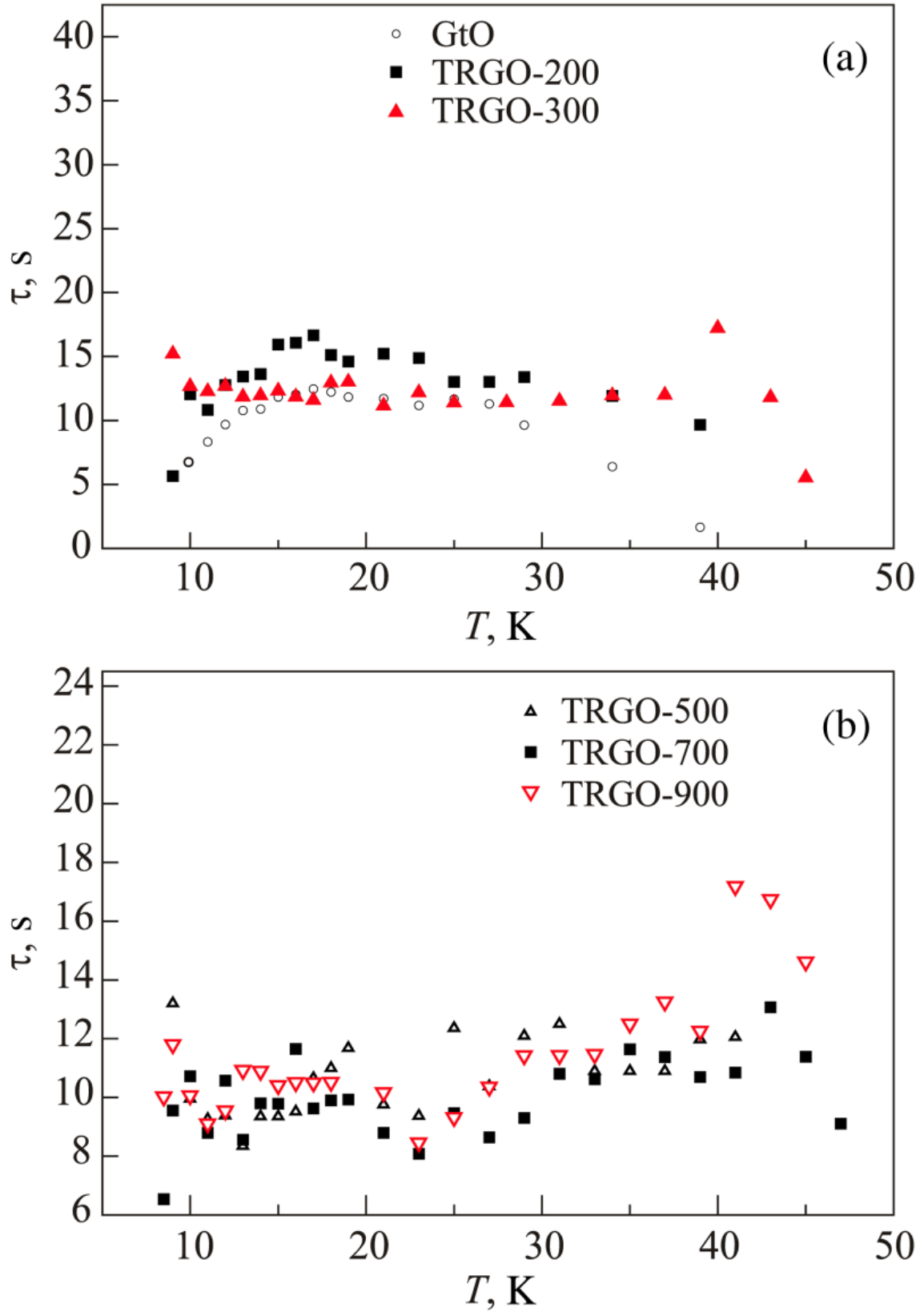


FIG. 3. Temperature dependences of the characteristic times of H_2 sorption by GtO, TRGO-200, and TRGO-300 samples (a); TRGO-500, TRGO-700, and TRGO-900 samples (b)

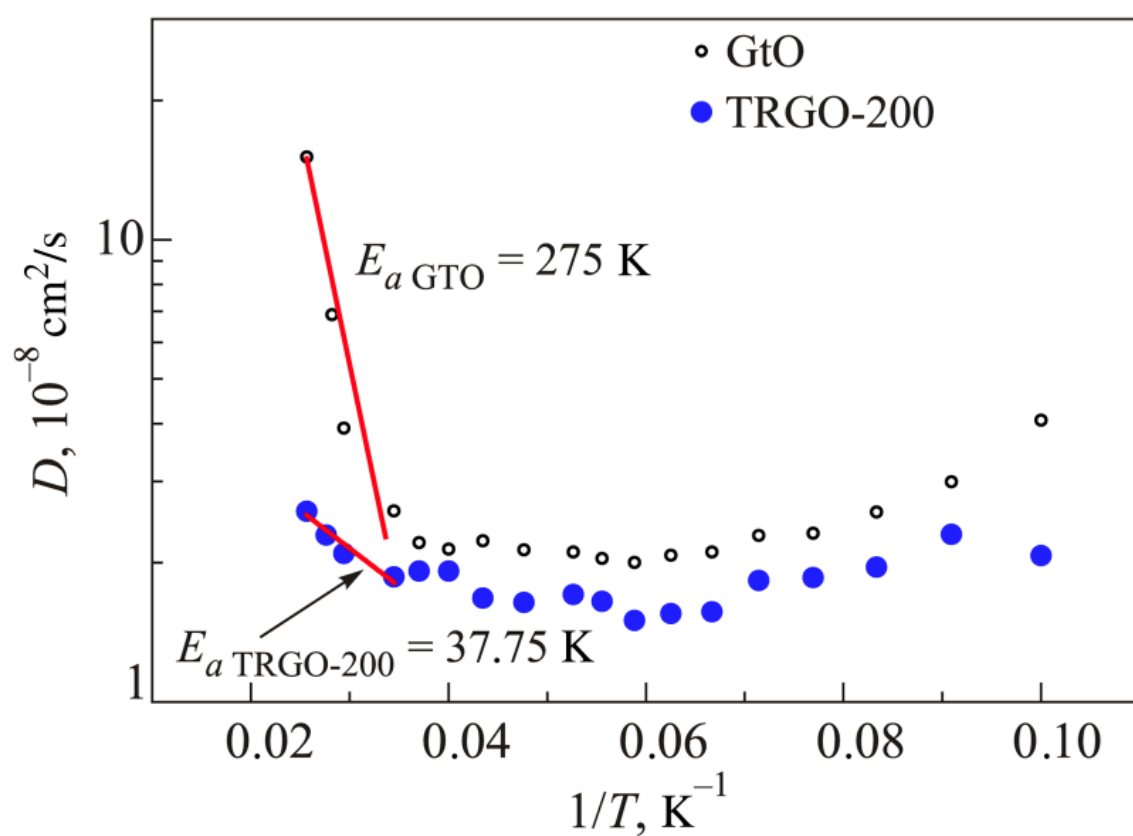


FIG. 4. Linear segments for $Y = \ln(D) - X = 1/T$ dependence for hydrogen diffusion coefficients in GtO and TRGO-200 samples.

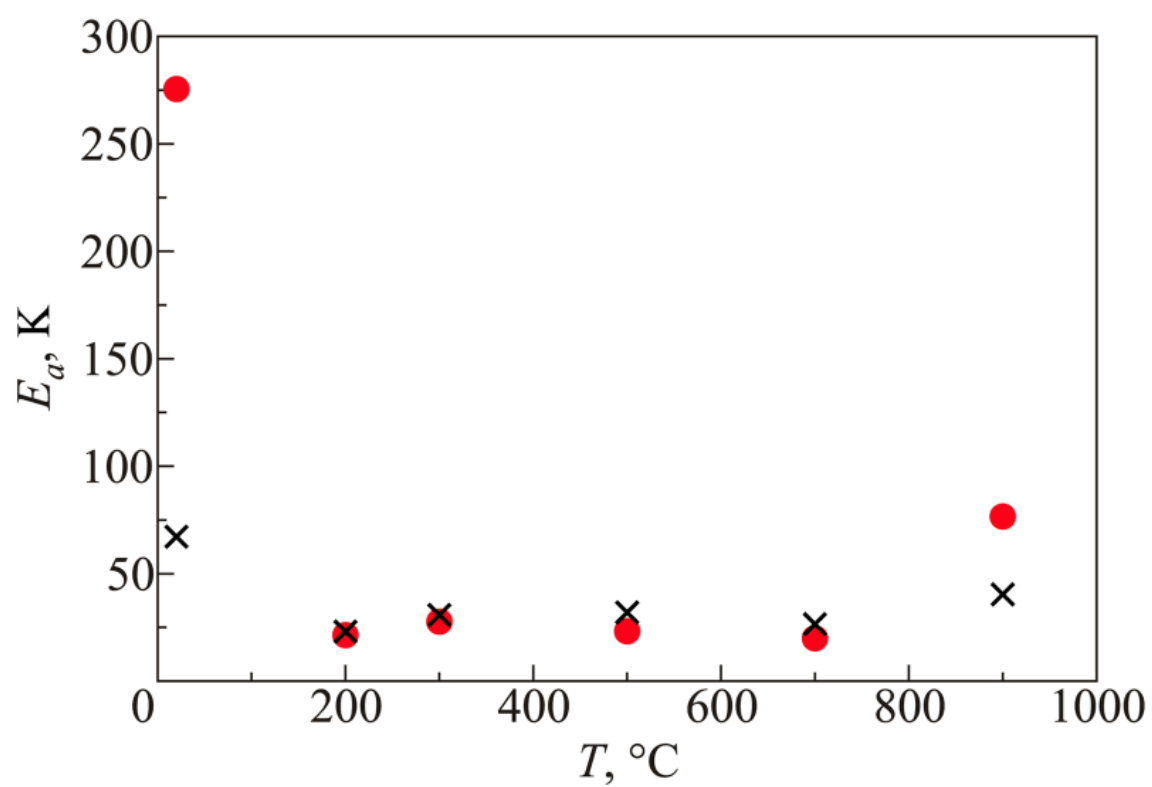


FIG. 5. Activation energy for hydrogen (●) and helium (x) diffusion²² vs. heat treatment temperature of graphene oxide.